AD-A064 429 AIR FORCE GEOPHYSICS LAB HANSCOM AFB MASS F/G 20/6
FORWARD SCATTER METER MEASUREMENTS OF SLANT VISUAL RANGE.(U)
AUG 78 W S HERING, E B GEISLER

UNCLASSIFIED AFGL-TR-78-0191 NL

END
DATE FILMED
4 -79
DDC

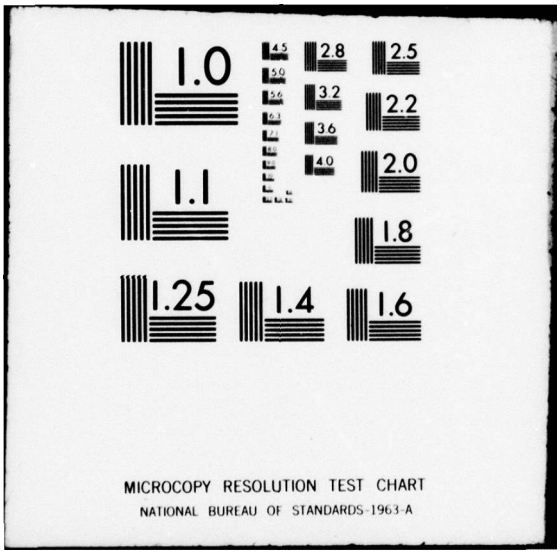
1.0
1.1
1.25
1.4
1.6
1.8
2.0
2.2
2.5
2.8
3.2
3.6
4.0
4.5
5.0
5.6
MICROCOPY RESOLUTION TEST CHART
NATIONAL BUREAU OF STANDARDS-1963-A

AFGL-TR-78-0191
AIR FORCE SURVEYS IN GEOPHYSICS, NO. 393

LEVEL II

Forward Scatter Meter Measurements of Slant Visual Range

WAYNE S. HERING
EDWARD B. GEISLER, Capt, USAF

9 August 1978

METEOROLOGY DIVISION PROJECT 6670
AIR FORCE GEOPHYSICS LABORATORY
HANSCOM AFB, MASSACHUSETTS 01731

AIR FORCE SYSTEMS COMMAND, USAF

This report has been reviewed by the ESD Information Office (OI) and is releasable to the National Technical Information Service (NTIS).

This technical report has been reviewed and is approved for publication.

FOR THE COMMANDER

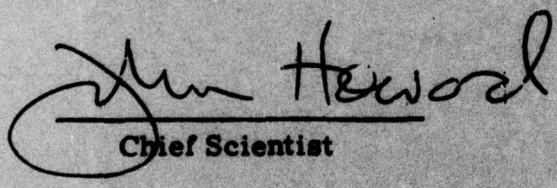

Chief Scientist

Qualified requestors may obtain additional copies from the Defense Documentation Center. All others should apply to the National Technical Information Service.

(9) Air Force surveys in geophysics,

Unclassified

SECURITY CLASSIFICATION OF THIS PAGE (When Data Entered)

REPORT DOCUMENTATION PAGE	READ INSTRUCTIONS BEFORE COMPLETING FORM
1. REPORT NUMBER: (14) AFGL-TR-78-0191, AFGL+AFSG-393	2. GOVT ACCESSION NO. / 3. RECIPIENT'S CATALOG NUMBER
4. TITLE (and Subtitle): (6) FORWARD SCATTER METER MEASUREMENTS OF SLANT VISUAL RANGE.	5. TYPE OF REPORT & PERIOD COVERED: Scientific. Interim.
	6. PERFORMING ORG. REPORT NUMBER: AFSG No. 393
7. AUTHOR(s): (10) Wayne S. Hering, Edward B. Geisler, Capt, USAF	8. CONTRACT OR GRANT NUMBER(s)
9. PERFORMING ORGANIZATION NAME AND ADDRESS: Air Force Geophysics Laboratory (LYU), Hanscom AFB, Massachusetts 01731	10. PROGRAM ELEMENT, PROJECT, TASK AREA & WORK UNIT NUMBERS: 62101F, 6670 1001, (16) 6670, (17) 10
11. CONTROLLING OFFICE NAME AND ADDRESS: Air Force Geophysics Laboratory (LYU), Hanscom AFB, Massachusetts 01731	(11) 12. REPORT DATE: 9 Aug 1978; 13. NUMBER OF PAGES: 38 (12) 29p.
14. MONITORING AGENCY NAME & ADDRESS (if different from Controlling Office)	15. SECURITY CLASS. (of this report): Unclassified; 15a. DECLASSIFICATION/DOWNGRADING SCHEDULE

16. DISTRIBUTION STATEMENT (of this Report)

Approved for public release; distribution unlimited.

17. DISTRIBUTION STATEMENT (of the abstract entered in Block 20, if different from Report)

18. SUPPLEMENTARY NOTES

19. KEY WORDS (Continue on reverse side if necessary and identify by block number)

Slant visual range
Visibility measurement
Airfield visibility
Runway visual range
Aircraft landing procedures

20. ABSTRACT (Continue on reverse side if necessary and identify by block number)

The potential for remote tower measurements of point visibility in the determination of slant range visibility for aircraft landing operations was explored through analysis of data collected at the Air Force Geophysics Laboratory Weather Test Facility at Otis AFB, Massachusetts. This report describes initial experiments that deal with an analysis of the small scale variability of extinction coefficient in time and space. Data from two instrumented towers spaced 1500 ft apart were classified for investigation of the horizontal variability of visibility at elevations up to 100 ft and space-time variability for

→ next page

DD FORM 1 JAN 73 1473 EDITION OF 1 NOV 65 IS OBSOLETE

Unclassified

SECURITY CLASSIFICATION OF THIS PAGE (When Data Entered)

409578 Jmc

20. (Cont)

lag periods from 0 to 10 minutes. The preliminary tests give additional evidence that the runway visual range (RVR) measurements alone often are not representative of pilot visibility during approach and touchdown. Remote measurements of visibility using either a 50-ft or 100-ft instrumented tower would add significantly to the real safety of "see-to-land" operations under conditions of Categories I, II, and IIIa through an improved description of conditions related to airfield visibility.

Preface

As part of a large field program, this work has benefited from the help of many people. The authors are especially grateful to Leo Jacobs, Ralph Hoar, and Clyde Lawrence, for establishing and maintaining the field test instrumentation; to John Ward, for assisting with the data processing; to Eugene Moroz, for many helpful discussions on the problems of visual range measurement; and to Helen Angier, for typing of the manuscript.

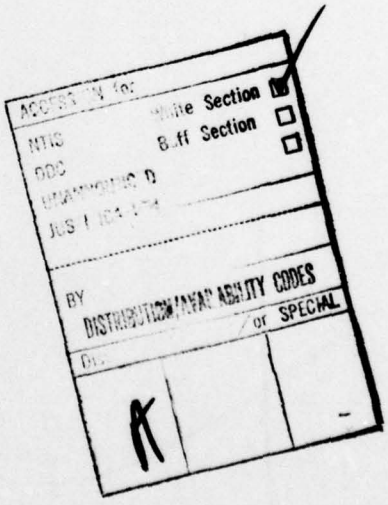

Contents

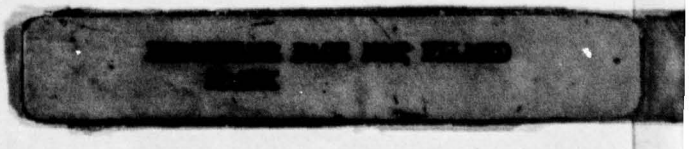

Illustrations

Tables

Forward Scatter Meter Measurements of Slant Visual Range

1. INTRODUCTION

Restricted visibility conditions continue to have a strong impact on the safety and efficiency of aircraft operations. However, improved low-visibility operational capability is being achieved through the installation of advanced instrument landing systems. Step by step the aviation industry has progressed to the point where a significant number of airfields have been approved for Category II operations. These airfields provide for instrument approaches to a decision height (DH) of 100 ft (30 m) with a runway visual range (RVR) minimum of 1200 ft (365 m). Inherently, the concept assumes that the pilot having made his decision to land has sufficient visual ground references at DH and sufficient time to make a safe landing. On the basis of the excellent safety record and widespread acceptance of Category II operations, even more sophisticated automated landing systems are being established to extend capability of operating in very low visibility conditions. The next step, Category IIIa operations, provides for landings with the aid of pilot visual reference under conditions when the RVR is not less than 700 ft (230 m).

The requirements for accurate and timely measurements of airfield visibility have become more urgent as the operational minima for low visibility approaches and landings are reduced. Current observational information supplied to the operator consists of human observer estimates of prevailing visibility and, at most major

(Received for publication 9 August 1978)

airfields, instrumental measurements of RVR at one or more locations adjacent to the runway. Although these observations supply essential information, experience has shown that the surface RVR measurements and general-area visibility observations often are not representative of the conditions encountered by the pilot as he proceeds along the glide path through the DH to touchdown. Progress has been difficult and slow in the development of effective techniques for the measurement of slant visual range (SVR) ahead of the aircraft, along and below the glide slope path. Two techniques for SVR measurement are under investigation by the Air Force Geophysics Laboratory (AFGL).[1] The first is an eye-safe lidar system employing a frequency doubled ruby laser. An experimental model of the single-ended lidar system is being fabricated by the Raytheon Company[2] based upon a novel optical design by HSS Inc.[3] Initial field tests of the lidar system have been delayed due to fabrication problems; these tests are now planned for the fall of 1978.

Meanwhile, field experiments with the second technique are well under way at the AFGL Weather Test Facility (WTF) at Otis AFB, Massachusetts. An instrumented tower approach is being evaluated that is similar in concept to a system proposed by the Federal Aviation Administration which was tested by Bradley, Lohkamp, and Williams.[4] The development and testing of SVR systems at the WTF are part of a continuing program to upgrade the Modular Automated Weather System (MAWS)[5] developed by AFGL for fixed-base Air Force requirements. The field tests of MAWS components, including the SVR system, involve a continuing series of detailed measurements of visual range at the WTF by means of forward scatter visibility meters and transmissometer instruments mounted both at the surface and on an array of instrumented towers. An automatic data acquisition system at the WTF processes the raw data in order to provide a continuous record of the fine scale variations of atmospheric extinction coefficient in time and space up to a height of 200 ft (60 m). The extensive data base provides a basis for assessment of many of the factors affecting our ability to measure and describe SVR in a variety of restrictive weather conditions. This report presents an interim summary of the investigation, with particular emphasis on the expected performance of a remote tower SVR system.

1. Moroz, E.Y. (1977) Investigation of Sensors and Techniques to Automate Weather Observations, AFGL-TR-77-0041, Instrumentation Paper No. 253.
2. McManus, R.G., Chabot, A.A., Young, R.M., and Novick, L.R. (1976) Slant Range Visibility Measuring Lidar, AFGL-TR-76-0262.
3. Stewart, H., Brower, W., and Shuler, M. (1976) Design Principles of a Slant Transmissometer for Airport Use, TuC6-1, Proceedings of Atmospheric Aerosols Conference, NASA CP-2004.
4. Bradley, G.S., Lohkamp, C.W., and Williams, R.W. (1976) Flight Test Evaluation of Slant Visual Range/Approach Light Contact Height (SVR/ALCH) Measurement System, Final Report Phase III, FAA-RD-76-167.
5. Tahnk, W.R., and Lynch, R.H. (1978) The Development of a Fixed Base Automated Weather Sensing and Display System, AFGL-TR-78-0009, Instrumentation Paper No. 260.

2. VISIBILITY MEASUREMENT TECHNIQUES

As reported by Douglas and Booker,[6] instrument-systems for RVR measurement have been used operationally in the United States for over two decades. The basic National Bureau of Standards (NBS) transmissometer instrument, the reference illuminance thresholds, and the concept of airfield visibility measurements have remained essentially unchanged since the systems first were installed at a selected group of Air Force bases in 1954, except for a shortening of the transmissometer baseline where necessary to extend the range of visibility measurement to lower values in support of Category II and Category III operations.

2.1 Runway Visual Range Measurement

The following definitions,* Runway Visual Range (RVR) and U.S. Definition of RVR, respectively, are given:

...The maximum distance in the direction of takeoff or landing at which the runway, or the specified lights or markers delineating it, can be seen from a position above a specified point on its center line at a height corresponding to the average eye-level of pilots at touchdown.

...A value normally determined by instruments located alongside and about 14 ft higher than the center line of the runway and calibrated with reference to the sighting of high-intensity runway lights or the visual contrast of other targets—whichever yields the greater visual range.

Thus the approved operational procedure is the measurement of the transmittance along an elevated horizontal path between the transmissometer source and the receptor. The recommended path length is 250 ft (75 m) for Category II operations. The transmittance t over baseline distance d is given by

$$t = e^{-bd}$$

where b is the atmospheric extinction coefficient which varies with the wavelength of light and the composition of the atmosphere.[7] In fog and precipitation conditions, the attenuation by absorption in the visible portion of the spectrum is small compared with attenuation by scattering, and therefore the extinction coefficient is given to a good first approximation by the atmospheric scattering coefficient alone.

---

6. Douglas, C.A., and Booker, R.L. (1977) Visual Range: Concepts, Instrumental Determination, and Aviation Applications, Final Report FAA-RD-77-8.

7. Middleton, W.E.K. (1952) Vision Through the Atmosphere, University of Toronto Press, Toronto.

*Federal Meteorological Handbook (1972) Government Printing Office, Washington, D.C., pp A6-304.

Thus the scattering coefficient is the primary atmospheric variable which determines the visibility. If b is relatively constant over a distance equal to visibility itself, the visual range V is related to the measurements of transmittance or scattering coefficient by Koschmieder's law when conventional daytime targets are used,

$$\epsilon_c = e^{-bV} = e^{(V \ln t)/d}$$

and by Allard's law (day or night) when lights are used as the reference,

$$\epsilon_t = \frac{Ie^{-bV}}{V^2} = \frac{Ie^{(V \ln t)/d}}{V^2}$$

where ϵ_c is the threshold of contrast and ϵ_t is the threshold illuminance. The RVR computer accepts the measured transmittance or extinction coefficient as input and calculates RVR in accordance with these relationships.

The operational values of threshold luminance ϵ_t (2 mi cd night and 1000 mi cd daytime) and contrast threshold ϵ_c (0.055 daytime) have been established through field experimentation. As such, they reflect the opposite effect of many influencing factors such as the luminance of the background, the physical characteristics of the target or light source, and observer knowledge of reference light or target location. These factors and other influences can lead to a wide spread in pilot perception of visual range relative to a given measured value of atmospheric extinction coefficient along the flight path.

To place requirements for accurate and representative measurements of atmospheric extinction coefficient in better perspective, let us consider the magnitude of the uncertainties that are caused by the factors in the foregoing discussion as revealed by the results of prior field experiments. For example, Figure 1 shows a cumulative frequency distribution of computed values of threshold illuminance based upon a series of visibility observations and corresponding measurements of transmittance carried out by Lefkowitz and Schlatter[8] at Atlantic City during fog conditions. Results of this study presented on probability paper show a roughly normal cumulative frequency distribution of the logarithm of illuminance threshold as determined from the carefully controlled experiment consisting of ground observations of runway edge lights and centerline lights from a fixed position 15 ft above the centerline of the runway. As shown in Figure 1, the standard deviation of $\log \epsilon_t$ for both day and night is about ± 1 or one order of magnitude in ϵ_t. This corresponds to about a 20 percent variation in RVR for visibility in the range 400

8. Lefkowitz, M., and Schlatter, E.E. (1966) An Analysis of Runway Visual Range, FAA-RD-66-100.

to 800 meters. It should be emphasized that those estimates of uncertainty in ϵ_t reflect, in part, sampling errors in extinction coefficient due to horizontal variations in fog density. Note that the 50-percent probability illuminance thresholds as given by these experimental data are near 100-mi cd for day and 1 mi-cd at night. Douglas and Booker[6] point out that to be applicable to the pilot these values should be increased by a factor of 2 or more to compensate for wind screen losses and the forward motion of the aircraft.

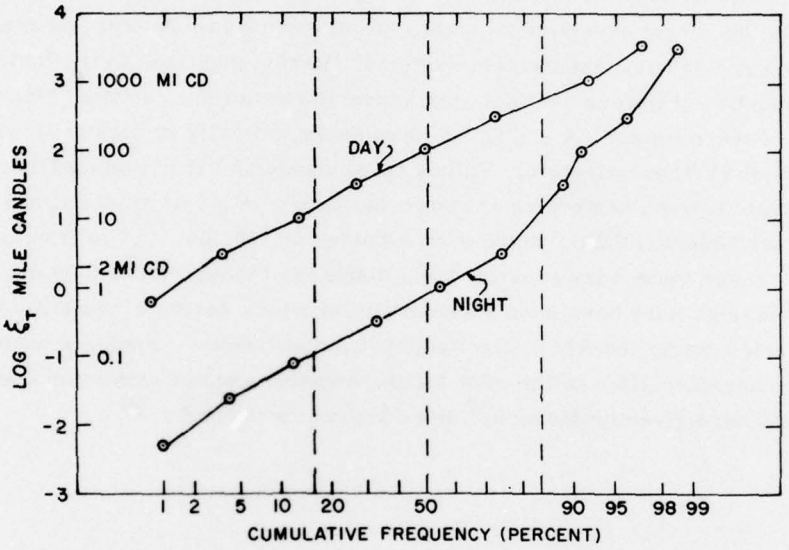

Figure 1. Cumulative Frequency of Day and Night Visual Illuminance Threshold as Determined in Atlantic City Experiments by Lefkowitz and Schlatter. The graph is a plot on probability paper of results given in Figure 20 (page 43) of their report (Reference 8). The number of night cases was 1049 and day cases totaled 894.

2.2 Slant Visual Range Measurement

With the foregoing limitations, similar concepts are applicable to SVR determination. The International Civil Aviation Organization defines SVR as "the furthest distance along the slant glide path at which approach lights are visible." The Federal Aviation Administration defines SVR more specifically as "the slant distance to the furthest high intensity runway edge light or approach light which a pilot will see at an altitude of 100 ft on the approach path or, if larger, the slant distance which would have a transmittance of 5.5 percent."[4]

A rigorous SVR system requires measurement of atmospheric extinction coefficient throughout the region below the glide path from flight altitude to the aim point. Thus, the degree of sophistication required in the remote sensing for SVR determination depends upon the inherent variability of extinction coefficient in time and space, which is the subject of the investigation described in the following sections.

3. TEST FACILITY INSTRUMENTATION AND MEASUREMENTS

The configuration of surface and tower mounted instruments at the WTF at Otis AFB, Massachusetts, continues to change in response to requirements for thermal fog dispersal experiments and to requirements for the test and evaluation of new meteorological measurement systems. Recent additions to the facility bring the total number of towers available for sensor installation to seven. Measurements from two of these towers, A and Q, as shown schematically in Figure 2, were used in this initial SVR investigation. Values of atmospheric extinction coefficient were derived from forward scatter measurements made with an array of F*G* and *G* Forward Scatter Meters (FSMs), which were mounted at 100, 50, and 10 ft on towers A and Q. These towers are separated by a distance of about 1500 ft (500 m). The FSM instruments have been used successfully in a long series of visibility experiments carried out by the Air Force Geophysics Laboratory. Analysis of the performance characteristics of the FSM for the measurement of extinction coefficient and visibility are given by Muench,[9] and Chisholm and Jacobs.[10]

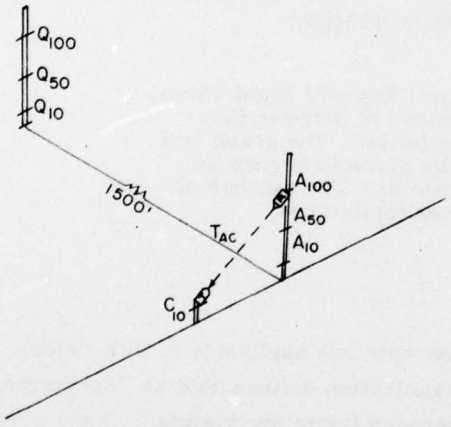

Figure 2. Configuration of Instrumented Towers and Location of Point Visibility Instruments Installed at the Otis AFB Weather Test Facility and Used for the SVR Tests

9. Muench, H. S., Moroz, E. Y., and Jacobs, L. P. (1974) Development and Calibration of the Forward Scatter Visibility Meter, AFCRL-TR-74-0145.

10. Chisholm, D. A., and Jacobs, L. P. (1975) An Evaluation of Scattering-Type Visibility Instruments, AFCRL-TR-75-0411, Instrumentation Paper No. 237.

The data acquisition system is automatic. It continuously records raw sensor output at the rate of five interrogations per minute. The raw data tapes are processed to yield a continuous time series composed of 1-min averages of extinction coefficient for each sensor. A sample of processed data acquired during a period of dense advection fog in April 1976 is shown in Figure 3. Three time series are shown presenting data from the 100-, 50-, and 10-ft levels of tower A. The sequence of data shows features that are characteristic of marine fog that has advected inland over the Cape Cod area. A quasi-steady state increase in advection fog density tends to be established and maintained as a result of fog droplet fallout and low-level

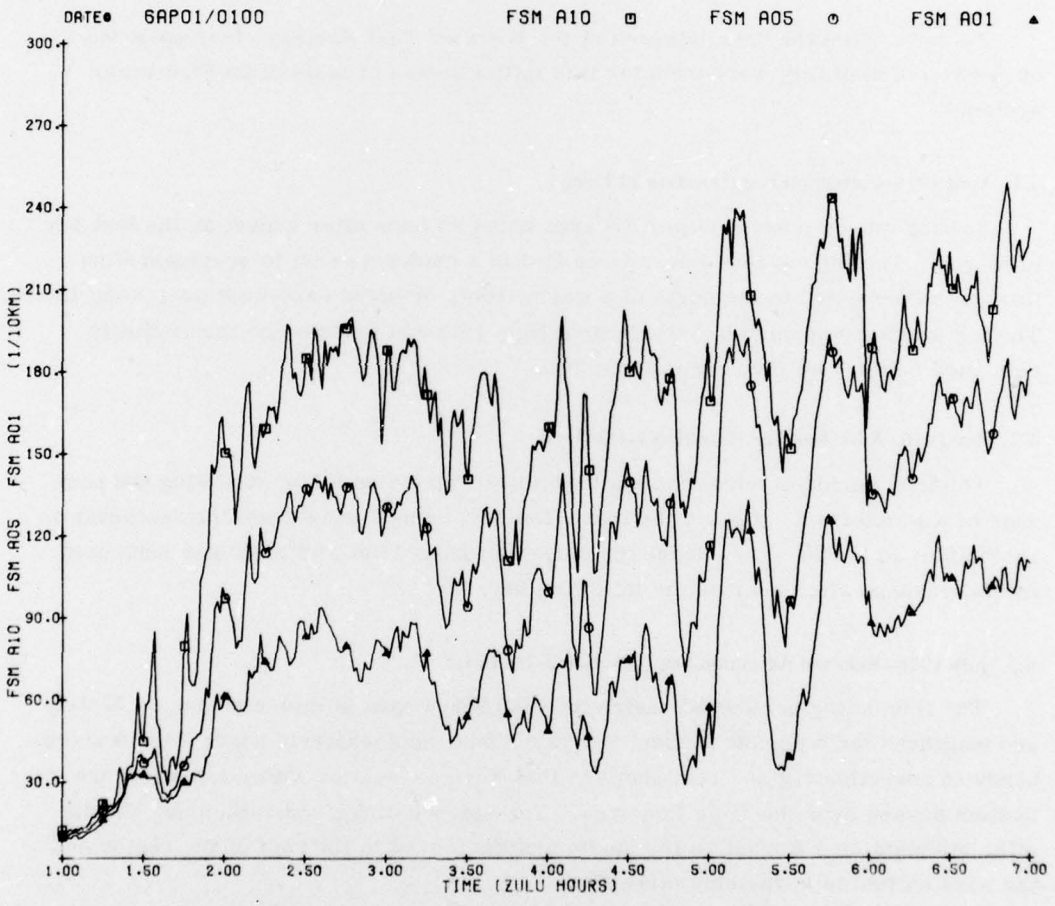

Figure 3. One-minute Average Values of Atmospheric Extinction Coefficient as Measured at the 10-, 50-, and 100-ft Levels of Tower A on 1 April 1976. Extinction coefficient is given in units of $10^4\ m^{-1}$

scavaging processes. The vertical correlation of even the high-frequency components remains high throughout the episode as the systematic vertical gradient is stubbornly maintained. As discussed by Roach,[11] the quasi-periodic oscillations in fog density, having in this case a period of about 35 min, probably are caused by an organized vertical motion pattern associated with gravity wave disturbances. Such fluctuations are a regular feature of Test Facility observations in advection fog situations.

4. TEST DATA

To date, from the data gathered at the Weather Test Facility, four episodes of restricted visibility were used for this initial series of tests of an FSM tower system:

4.1 April 1976—Advection Fog (Duration 11 Hours)

Sea fog moved into the Otis AFB area about an hour after sunset on the last day in March. The fog advanced over Cape Cod in a moderate east to southeast wind flow which persisted to the north of a warm front, oriented east-west near Long Island. The fog was accompanied by intermittent light rain and drizzle and the visibility remained below 2 mi throughout the night.

4.2 May 1976—Advection Fog (Duration 1-1/2 Days)

The long period of advection fog began near sunset on 2 May following the passage of a warm front. Behind the front, low level winds were from the southeast or south 10 to 20 knots. Very dense fog persisted from 1400 LST on 2 May until cold frontal passage after sunrise the following day.

4.3 July 1976—Rain and Advection Fog (Duration 2-7/8 Days)

The fluctuating periods of restricted visibility began in mid-morning on 29 July and continued for a period of about 3 days. Under southeasterly winds 8 to 15 knots, bands of advection fog and rain showers that were associated with a low pressure system passed over the Cape Cod area. The episode of fog and rain ended shortly after midnight on 1 August as the storm system moved to the east of the region and the wind shifted to a westerly direction.

---

11. Roach, W. T. (1976) On some quasi-periodic oscillations observed during a field investigation of radiation fog, Quart. J. Roy. Meteorol. Soc. 102:355-360.

4.4 August 1977—Radiation Fog (Duration 7 Hours)

Dense radiation fog formed during the night of 22 to 23 August following the passage of a cold front over Cape Cod which was accompanied by heavy rain showers. Under clearing skies and radiational cooling, a strong low-level temperature inversion was formed a few hours after sunset. Radiation fog was observed before midnight and persisted until after sunrise. Local wind speeds remained less than 3 knots throughout the night and increased to 8 to 10 knots in association with clearing fog conditions at 0600 LST.

5. FORWARD SCATTER METER TOWER EXPERIMENTS

For purposes of this initial study, a straightforward average of the FSM measurements at tower A up to the 100-ft level was assumed representative of the SVR in the simulated approach zone:

$$\overline{A} = (A_{100} + A_{50} + A_{10})/3 .$$

The objective was to determine the accuracy with which $\overline{A}$ could be specified at specific time intervals from time zero to plus 10 min from various combinations of FSM measurements made at time zero at remote tower Q (see Figure 2). Forward Scatter Meter measurements at A_{10} were also used as predictors, recognizing that measurements from the touchdown RVR instrument would be available for SVR determination as part of an automated airfield observing system.

Specific combinations of measurements from Q_{100}, Q_{50}, Q_{10}, and A_{10} were preselected as predictors of $\overline{A}$. The series of predictors were chosen to investigate specification accuracy relative to the number and spacing of the instruments as follows:

Method 1. Installation of a 100-ft tower and 3 FMS instruments:

$$\overline{A} = (Q_{100}, Q_{50}, Q_{10}) = (Q_{100} + Q_{50} + Q_{10})/3 + \delta$$

Method 2. Installation of a 50-ft tower with one FSM instrument mounted at the 50-ft level and measurements from the touchdown RVR instrument:

$$\overline{A} = (Q_{50}Q_{10}) = k_1 Q_{50} + k_q A_{10} + \delta$$

Method 3. Measurements from the existing touchdown RVR instrument:

$$\overline{A} = A_{10} + \delta$$

Because of the limited data base available for this initial series of tests, simplifying assumptions were made to establish in advance the specification algorithms. Method 1 assumes horizontal homogeneity of fog density over the 1500-ft distance between towers Q and A. The Method 2 prediction algorithm is a linear combination of measurements from the 50-ft level of remote tower Q and surface measurements from the touchdown RVR instrument, taken as A_{10}. Estimates of coefficients k_1 and k_2 were obtained through multiple linear regression techniques using a small sample of data obtained prior to the onset of the test period in advection fog conditions. No attempt was made to refine the coefficients during this preliminary study; thus k_1 and k_2 were held constant irrespective of the cause of restricted visibility (rain, shallow ground fog, advection fog, and so on). Method 3 was included as a baseline reference. This method measures the representativeness of an RVR measurement as an estimate of visual range over a 100-ft vertical column overhead.

6. EVALUATION CRITERIA

Forecasts of vertically averaged extinction coefficient $\bar{A}$ by the three provisional methods were verified separately for each episode and several lags, using a variety of established measures of accuracy. The percent root-mean-square error is given by

$$PE = \left[\frac{1}{n} \sum_{i=1}^{n} \left(\frac{\hat{\bar{A}}_i - \bar{A}_i}{\bar{A}_i} \right)^2 \right]^{1/2} \times 100$$

where $\hat{\bar{A}}_i$ is the forecasted or estimated value and $\bar{A}_i$ is the observed. Pairs of values where $\bar{A}_i \leq 1\ km^{-1}$ (nighttime RVR > 4 mi) were excluded from the sample to eliminate spurious values of PE that can occur during periods of relatively good visibility (denominator near zero).

Another series of verification scores related to the practical utility of the methods for prediction of below-limit SVR conditions were determined through calculation of 2 × 2 contingency tables for two thresholds of average extinction coefficient $\bar{A}$. One threshold, $5\ km^{-1}$, converts through Allard's law at Runway Light Setting 5 to a visual range of about 1/2 mi (800 m) daytime and 1 mi (1600 m) at night. The second threshold of $12\ km^{-1}$ corresponds to about 1/4 mi (400 m) daytime and 1/2 mi (800 m) at night.

Shown for example in Figure 4 is the resultant contingency table as calculated for the 1 April 1976 fog episode using $Q_{100}Q_{50}Q_{10}$ as a zero lag predictor of $\bar{A}$ above

or below a nighttime threshold of 12 km^{-1}. Using values in Figure 4 for illustration, one notes that verification scores were calculated as follows:

1. Probability of Detection (POD)

$$POD = \frac{268}{284} \times 100 = 94.4\%$$

2. False Alarm Ratio (FAR)

$$FAR = \frac{15}{283} \times 100 = 5.3\%$$

3. Threat Score (TS)

$$TS = \frac{268}{(268+15+16)} \times 100 = 89.6\%$$

	FORECAST		
OBSERVED	$\bar{A} \geq 12$ km^{-1} VISIBILITY BELOW LIMIT	$\bar{A} < 12$ km^{-1} VISIBILITY ABOVE LIMIT	TOTAL MIN
VISIBILITY BELOW LIMIT $\bar{A} \geq 12$ km^{-1}	268	16	284
VISIBILITY ABOVE LIMIT $\bar{A} < 12$ km^{-1}	15	362	377
TOTAL MIN	283	378	661

Figure 4. Contingency Table for the 1 April 1976 Fog Episode Which Illustrates Method of Computing Verification Scores. The example refers to the extinction coefficient threshold of 12 km^{-1} which corresponds to a visual range of about 400 m (1/4 mi) in the daytime and 800 m (1/2 mi) at night

7. DISCUSSION OF RESULTS

Some important generalizations can be made on the effectiveness of a FSM tower system for SVR determination in a coastal region such as Cape Cod. In particular, the remote tower measurements provide accurate estimates of approach zone conditions in sea fog situations. Minute by minute comparisons of specific vs observed values of $\bar{A}$ for the 1 April 1976 case are shown in Figure 5 for both Method 1 and Method 2. Under the breezy wind conditions which usually accompany the advection fog on the Massachusetts coast, the fog density tends to be uniform over distances comparable to that between remote tower Q and tower A (1500 ft), so that the remote FSM measurements closely track the observed conditions in the simulated approach zone, including significant fluctuations occurring on a time scale of a few minutes. Both Methods 1 and 2 closely specify the time of onset and end of periods of below-limit visibility at tower A in sea fog conditions.

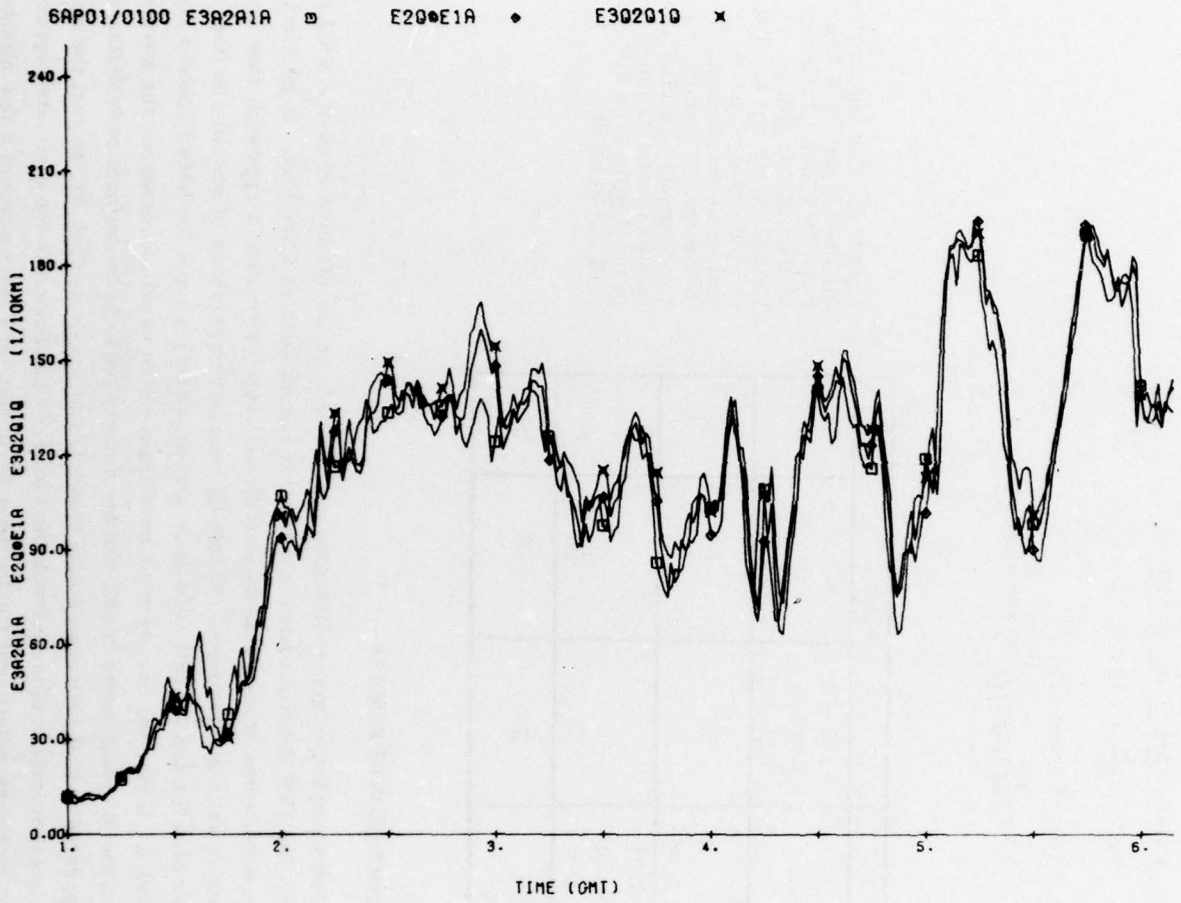

Figure 5. Observed and Specified One-Minute Values of Extinction Coefficient ($\bar{A}$) for a 6-hr Period During the Fog Episode of 1 April 1976. The number E3Q2Q1Q refers to specification Method 1, based on point visibility measurements at 3 levels of remote tower Q; E2QE1A refers to Method 2 based upon measurements at Q_{50} and A_{10}; E3A2A1A refers to the predictand, which is the average of measurements from the 3 levels of tower A

Verification values of percent rms error (PE) given in Table 1 reflect the consistently good performance of Methods 1 and 2 in advection fog situations. For the three sea fog episodes, values of PE are less than 20 percent at zero lag and only slightly higher at 2 minutes. The percentage errors for Methods 1 and 2 increase substantially at longer forecasting intervals, becoming about a factor of 2 higher than the zero lag values after 5 minutes. As expected, much larger errors were observed in the radiation fog case because of the patchy nature of this type of fog which forms under conditions of high moisture at low levels of the atmosphere, clear skies, and light winds. Notice that the PE values for the August episode were about 40 percent at 0 to 2 min for the methods based upon the remote tower measurements. It is of special interest that the errors for both advection and radiation fog resulting from the use of the 50-ft tower (Method 2) were virtually the same as those using a 100-ft tower system with 3 FSM instruments (Method 1), even though the provisional coefficients k_1 and k_2, for Method 2 were derived from a small data sample. In turn, the two tower-based methods represent a substantial improvement over control Method 3 which uses the RVR measurement at A_{10} as a predictor of slant visual range. A strong bias exists in the Method 3 forecast errors which changes sign, depending upon the type of fog conditions. A strong increase in fog density with increasing height is observed in advection fog and the reverse is true of radiation or ground fog conditions.

Further evidence of the excellent potential of remote-tower FSM measurements for timely discrimination of approach zone visibility in coastal sea fog conditions is given by the test scores for probability of detection (POD), false alarm ratio (FAR) and threat score (TS) listed in Tables 2 through 4). The minute by minute POD of below limit visibility, as defined by the two preselected threshold values of $\overline{A}$, exceeds 90 percent for all 3 advection fog cases for both zero and 2-min lag periods. The POD for $\overline{A}$ greater than 5 km^{-1} (less than 1/2 mi visual range in the daytime) averages slightly higher than the POD for $\overline{A}$ greater than 12 km^{-1} threshold (less than 1/4 mi daytime visual range). The test scores of POD for Methods 1 and 2 were particularly high, 98 percent or greater for the 5 km^{-1} threshold for the April and May advection fog episodes.

Some additional items of interest in Tables 2 through 4 are as follows:

(1) The POD of below limit visibility decreases significantly in some advection fog cases at lag periods greater than 2 minutes. Thus, an effective automated system for rapid dissemination and display of the observations is essential.

(2) As shown in Table 3, Methods 1 and 2, using remote tower measurements, have low false-alarm ratios for lag times up to 2 min or more. On the other hand, Method 3, based upon surface RVR measurements, consistently overestimates the fog density above the surface in radiation fog; hence the high false-alarm ratios for the August case.

(3) Since in most instances the false-alarm ratios are low for Methods 1 and 2, it follows that the Threat Scores (TS) in Table 4 closely parallel the POD values given in Table 2 and, for at least the short lag periods, are only a few percent lower than the corresponding POD values.

Table 1. Values of Percent Root-Mean-Square Error for Forecasts Made by the Three Methods for Each Fog Episode

Method	Episode	Lag (Minutes)			
		0	2	5	10
1. $Q_{100}Q_{50}Q_{10}$	1 Apr 76 Ad Fog	11	18	27	38
	July 76 Rain/Ad Fog	17	23	39	60
	May 76 Ad Fog	19	21	25	47
	Aug 77 Rad Fog	42	43	43	42
2. $Q_{50}A_{10}$	1 Apr 76 Ad Fog	12	16	23	33
	July 76 Rain/Ad Fog	14	20	34	54
	May 76 Ad Fog	18	21	27	51
	Aug 77 Rad Fog	38	41	51	81
3. A_{10}	1 Apr 76 Ad Fog	43	44	43	45
	July 76 Rain/Ad Fog	34	36	41	50
	May 76 Ad Fog	33	34	36	38
	Aug 77 Rad Fog	114	139	203	331

Table 2a. Values of Probability of Detection for Forecasts Made by the Three Methods for the Four Fog Episodes (Percent) (Threshold = 12 km^{-1})

Method	Episode	Lag (Minutes)			
		0	2	5	10
1. $Q_{100}Q_{50}Q_{10}$	1 Apr 76 Ad Fog	94	90	83	71
	July 76 Rain/Ad Fog	97	96	91	83
	May 76 Ad Fog	97	97	97	94
	Aug 77 Rad Fog	80	80	80	79
2. $Q_{50}A_{10}$	1 Apr 76 Ad Fog	91	88	80	69
	July 76 Rain/Ad Fog	91	90	86	79
	May 76 Ad Fog	97	96	96	94
	Aug 77 Rad Fog	78	78	78	78
3. A_{10}	1 Apr 76 Ad Fog	13	13	13	12
	July 76 Rain/Ad Fog	56	56	56	54
	May Ad Fog	87	87	87	87
	Aug 77 Rad Fog	100	100	100	98

Table 2b. Values of Probability of Detection for Forecasts Made by the Three Methods for the Four Fog Episodes (Percent) (Threshold = 5 km^{-1})

Method	Episode	Lag (Minutes)			
		0	2	5	10
1. $Q_{100}Q_{50}Q_{10}$	1 Apr 76 Ad Fog	98	97	96	95
	July 76 Rain/Ad Fog	95	94	89	85
	May 76 Ad Fog	99	99	98	97
	Aug 77 Rad Fog	66	66	66	66
2. $Q_{50}A_{10}$	1 Apr 76 Ad Fog	96	95	95	93
	July 76 Rain/Ad Fog	84	83	80	76
	May 76 Ad Fog	98	98	96	96
	Aug 77	98	98	96	92
3. A_{10}	1 Apr 76 Ad Fog	72	72	72	72
	July 76 Rain/Ad Fog	48	47	46	45
	May 76 Ad Fog	86	85	85	85
	Aug 77 Rad Fog	100	99	99	98

Table 3a. Values of False Alarm Ratio for Forecasts Made by the Three Methods for Each Fog Episode (Percent) (Threshold = 12 km^{-1})

Method	Episode	Lag (Minutes)			
		0	2	5	10
1. $Q_{100}Q_{50}Q_{10}$	1 Apr 76 Ad Fog	5.3	9.5	28.6	38.9
	July 76 Rain/Ad Fog	3.9	5.0	9.6	17.3
	May 76 Ad Fog	1.9	2.1	2.5	4.7
	Aug 77 Rad Fog	0.0	0.0	0.0	0.7
2. $Q_{50}A_{10}$	1 Apr 76 Ad Fog	3.3	6.7	14.9	26.5
	July 76 Rain/Ad Fog	0.4	1.7	6.7	13.9
	May 76 Ad Fog	0.2	0.7	1.4	3.2
	Aug 77 Rad Fog	0.0	0.0	0.0	0.0
3. A_{10}	1 Apr 76 Ad Fog	0.0	0.0	0.0	10.5
	July 76 Rain/Ad Fog	0.0	0.0	0.0	3.4
	May 76 Ad Fog	0.0	0.0	0.0	0.0
	Aug 77 Rad Fog	26.1	26.1	26.1	27.7

Table 3b. Values of False Alarm Ratio for Forecasts Made by the Three Methods for Each Fog Episode (Percent) (Threshold = 5 km^{-1})

Method	Episode	Lag (Minutes)			
		0	2	5	10
1. $Q_{100}Q_{50}Q_{10}$	1 Apr 76 Ad Fog	1.8	2.8	3.9	5.6
	July 76 Rain/Ad Fog	7.7	8.2	13.8	18.1
	May 76 Ad Fog	0.0	0.0	0.1	2.2
	Aug 77 Rad Fog	0.0	0.0	0.0	0.0
2. $Q_{50}A_{10}$	1 Apr 76 Ad Fog	0.0	0.4	1.3	3.0
	July 76 Rain/Ad Fog	1.7	3.1	7.8	13.1
	May 76 Ad Fog	0.3	0.4	0.8	1.9
	Aug 77 Rad Fog	0.0	0.8	3.3	7.0
3. A_{10}	1 Apr 76 Ad Fog	0.0	0.0	0.0	0.0
	July 76 Rain/Ad Fog	0.0	1.7	5.3	8.3
	May 76 Ad Fog	0.0	0.1	0.3	0.6
	Aug 77 Rad Fog	9.9	10.3	10.6	12.1

Table 4a. Values of Threat Score for Forecasts by the Three Methods for Each Fog Episode (Percent) (Threshold = 12 km^{-1})

Method	Episode	Lag (Minutes)			
		0	2	5	10
1. $Q_{100}Q_{50}Q_{10}$	1 Apr 76 Ad Fog	90	82	71	55
	July 76 Rain/Ad Fog	93	91	83	71
	May 76 Ad Fog	95	95	94	90
	Aug 77 Rad Fog	80	80	80	79
2. $Q_{50}A_{10}$	1 Apr 76 Ad Fog	88	82	70	55
	July 76 Rain/Ad Fog	91	89	81	70
	May 76 Ad Fog	97	96	94	91
	Aug 77 Rad Fog	78	78	78	78
3. A_{10}	1 Apr 76 Ad Fog	13	13	13	12
	July 76 Rain/Ad Fog	56	56	56	53
	May 76 Ad Fog	87	87	87	87
	Aug 77 Rad Fog	74	74	74	71

Table 4b. Values of Threat Score for Forecasts by the Three Methods for Each Fog Episode (Percent) (Threshold = 5 km^{-1})

Method	Episode	Lag (Minutes)			
		0	2	5	10
1. $Q_{100}Q_{50}Q_{10}$	1 Apr 76 Ad Fog	97	95	93	90
	July 76 Rain/Ad Fog	88	87	78	72
	May 76 Ad Fog	99	98	98	95
	Aug 77 Rad Fog	66	66	66	66
2. $Q_{50}A_{10}$	1 Apr 76 Ad Fog	96	95	93	90
	July 76 Rain/Ad Fog	83	81	75	68
	May 76 Ad Fog	98	98	97	95
	Aug 77 Rad Fog	97	97	93	86
3. A_{10}	1 Apr 76 Ad Fog	72	72	72	72
	July 76 Rain/Ad Fog	48	47	45	43
	May 76 Ad Fog	86	85	85	85
	Aug 77 Rad Fog	90	89	89	86

For operational purposes, it may be sufficient to establish an observational capability which simply specifies whether or not below-limit visibility conditions exist at an airfield with respect to either the RVR threshold value or the SVR threshold value. As noted, radiation fog density characteristically decreases with height above the surface so that the RVR consistently is lower than the corresponding SVR. Thus, we can rely on surface visibility instruments alone to detect the onset and continued presence of below-limit conditions during episodes of radiation fog. To the extent that radiation fog conditions prevail with RVR less than SVR, it is not so important to monitor closely the visibility conditions aloft as long as the more critical RVR is described accurately by the surface visibility instruments. This is fortunate because SVR discrimination is difficult in radiation fog conditions due to the large horizontal variability in fog density.

On the other hand, it is the SVR measurement that is of major interest in advection fog conditions that prevail in coastal regions. Since sea fog density increases with height, below-limit SVR typically occurs first and persists longer than RVR less than the same threshold value. As revealed by the initial field experiments, SVR in advection fog is described effectively by means of remote tower measurement of point visibility.

8. CONCLUSIONS

The extensive array of point visibility meters installed at the Weather Test Facility at Otis AFB, Massachusetts, provides the basis for detailed investigation of the small-scale variability of visibility in time and space up to 200 ft above the surface. Preliminary analysis of data collected during the first year of operation demonstrates the importance of measurements above ground level for meaningful description of visibility conditions in support of aircraft landing operations. Measurements aloft up to decision height are of special importance in coastal advection fog conditions since the SVR along the elevated glide slope is predominantly lower than indicated by surface runway visual range measurements. In advection fog conditions observed at Cape Cod, preliminary results indicate that a 50-ft remote tower system would provide a probability of detection of below-limit SVR of greater than 90 percent as compared with large uncertainties in SVR discrimination with conventional RVR measurements alone.

Follow-on studies of SVR measurement will deal with a more complete definition of slant visual range derived from simultaneous measurements from several instrumented towers in the simulated approach zone established at the Otis AFB Weather Test Facility. Provisional algorithms have been developed for the short-range prediction of SVR using remote tower visibility measurements. The

algorithms are under continuing evaluation at the Test Facility and they have been integrated into the demonstration model of MAWS at Scott AFB, Illinois.

References

1. Moroz, E.Y. (1977) Investigation of Sensors and Techniques to Automate Weather Observations, AFGL-TR-77-0041, Instrumentation Paper No. 253.
2. McManus, R.G., Chabot, A.A., Young, R.M., and Novick, L.R. (1976) Slant Range Visibility Measuring Lidar, AFGL-TR-76-0262.
3. Stewart, H., Brower, W., and Shuler, M. (1976) Design Principles of a Slant Transmissometer for Airport Use, TuC6-1, Proceedings of Atmospheric Aerosols Conference, NASA CP-2004.
4. Bradley, G.S., Lohkamp, C.W., and Williams, R.W. (1976) Flight Test Evaluation of Slant Visual Range/Approach Light Contact Height (SVR/ALCH) Measurement System, Final Report Phase III, FAA-RD-76-167.
5. Tahnk, W.R., and Lynch, R.H. (1978) The Development of a Fixed Base Automated Weather Sensing and Display System, AFGL-TR-78-0009, Instrumentation Paper No. 260.
6. Douglas, C.A., and Booker, R.L. (1977) Visual Range: Concepts, Instrumental Determination, and Aviation Applications, Final Report FAA-RD-77-8.
7. Middleton, W.E.K. (1952) Vision Through the Atmosphere, University of Toronto Press, Toronto.
8. Lefkowitz, M., and Schlatter, E.E. (1966) An Analysis of Runway Visual Range, FAA-RD-66-100.
9. Muench, H.S., Moroz, E.Y., and Jacobs, L.P. (1974) Development and Calibration of the Forward Scatter Visibility Meter, AFCRL-TR-74-0145.
10. Chisholm, D.A., and Jacobs, L.P. (1975) An Evaluation of Scattering-Type Visibility Instruments, AFCRL-TR-75-0441, Instrumentation Paper No. 237.
11. Roach, W.T. (1976) On some quasi-periodic oscillations observed during a field investigation of radiation fog, Quart. J. Roy. Meteorol. Soc. 102:355-360.